scientific reports

Check for updates

OPEN

1-Palmitoyl-2-linoleoyl-3-acetyl-rac-glycerol (PLAG) enhances the therapeutic and immunological efficacy of high-dose radiotherapy in preclinical tumor models

Hyunkyung Kim[1,4], Haeun Cho[1,4], Sojung Sun[1], Tae-Jin Kim[2], Kwangmo Yang[1], Won Il Jang[1], Seok-Joo Chun[3] & Mi-Sook Kim[1]✉

1-Palmitoyl-2-linoleoyl-3-acetyl-rac-glycerol (PLAG) is a synthetic monoacetyldiglyceride known for its immunomodulatory properties, including regulation of pathological neutrophil trafficking and modulation of antitumor immune responses. In this study, we evaluated the therapeutic potential of PLAG as an adjuvant to high-dose radiotherapy using murine tumor models. Combination treatment with PLAG and radiotherapy significantly delayed tumor growth in immunocompetent mice, whereas this therapeutic benefit was absent in immunodeficient hosts, indicating an immune-dependent mechanism. While PLAG selectively enhance CD8⁺ T-cell functional activation when combined with radiotherapy compared to radiotherapy alone, as evidenced by increased numbers of INF-γ⁺, Granzyme B⁺, and effector memory CD8⁺ T-cells. PLAG sustained tumor antigen-specific INF-γ secretion of splenocytes after radiotherapy, indicating prolonged systemic immune activation. Importantly, the amplified systemic immune response translated into a robust abscopal effect. In conclusion, these findings suggest that PLAG amplifies and sustains radiotherapy-induced antitumor immunity by increasing functional activation of CD8⁺ T-cells, and may serve as a promising immunomodulatory adjuvant to improve radiotherapy outcomes.

Keywords PLAG (1-Palmitoyl-2-linoleoyl-3-acetyl-rac-glycerol), High-dose radiotherapy, Antitumor immunity, CD8⁺ T-cells, Immunomodulatory adjuvant

1-Palmitoyl-2-linoleoyl-3-acetyl-rac-glycerol (PLAG), also known as EC-18, is a chemically synthesized monoacetyldiglyceride originally derived from sika deer antlers[1,2]. PLAG was granted Orphan Drug Designation by the U.S. Food and Drug Administration (FDA) in 2018 for the treatment of acute radiation syndrome (ARS)[3]. Recent preclinical studies have further highlighted the immune-modulating potential of PLAG under various inflammatory conditions[4,5]. PLAG has been shown to regulate neutrophil trafficking, modulate myeloid cell activity, and protect epithelial integrity in models of gastrointestinal or pulmonary radiation injury[3,6]. While, in murine tumor models, PLAG inhibits aberrant neutrophil infiltration in the tumor microenvironment, mitigating excessive inflammation and promoting CD8⁺ T-cell-mediated antitumor responses[4]. Importantly, the favorable safety and tolerability of PLAG have also been validated in a recent randomized Phase II clinical trial, supporting its translational potential as an immune modulating agent with a favorable tolerability in combination with cancer therapies[7]. The PLAG concentration in preclinical model differs between in anti-inflammatory settings and inducing alterations within the tumor microenvironment. For instance, PLAG doses ranging from 50 to 500 mg/kg have been employed in radiation injury and systemic inflammation models to mitigate hematopoietic ARS or gastrointestinal toxicity, often showing dose-dependent improvements in cell recovery and survival outcomes[8]. In particular, studies evaluating the protective role of PLAG against gastrointestinal ARS administered 250 mg/kg daily to alleviate crypt and villus damage and restore intestinal function in total-body irradiated mice[3]. In tumor models, doses between 50 and 100 mg/kg of PLAG effectively regulated neutrophil

[1]Department of Radiation Oncology, Korea Institute of Radiological & Medical Sciences, 75 Nowon–ro, Nowon–gu, Seoul, Korea. [2]Department of Radiation Biomedical Research, Korea Institute of Radiological & Medical Sciences, Seoul, Korea. [3]Department of Radiation Oncology, Ilsan Dongguk University Hospital, Goyang, Korea. [4]These authors contributed equally to this work: Hyunkyung Kim and Haeun Cho. ✉email: mskim@kirams.re.kr

infiltration and promoted antitumor immune responses without inducing systemic toxicity[4]. In this study, we adopted a dose of 250 mg/kg to effectively evaluate the adjuvant potential of PLAG in combination with high-dose radiotherapy, while ensuring it did not introduce additional systemic toxicity.

Conventional fractionated radiotherapy (CFR) remains one of the most extensively employed therapeutic modalities for the management of solid tumors, achieving effective local tumor control primarily through the induction of DNA damage and subsequent tumor cell death[9,10]. While, systemic effects such as abscopal responses are infrequently observed[11–13]. With advances in imaging and radiation delivery technologies, high-dose hypofractionated approaches such as stereotactic ablative radiotherapy (SABR) have been increasingly adopted in clinical practice. These regimens not only offer superior local control in selected tumor types but also enhance immunogenic cytotoxicity and possess the potential to elicit abscopal effects compared to CFR[14,15]. Radiation-induced immunogenic cell death promotes the release of tumor-associated antigens and danger signals, upregulation of MHC molecules, and recruitment of antigen-presenting cells, thereby priming cytotoxic $CD8^+$ T-cells[13,14,16–18]. Activated $CD8^+$ T-cells can mediate tumor regression beyond the irradiated field, representing the immunological basis of the abscopal effect[12]. However, the immunostimulatory capacity of radiotherapy is often counterbalanced by radiation-induced immunosuppressive mechanisms, including the expansion of regulatory T cells (Tregs), myeloid-derived suppressor cells (MDSCs), and tumor-associated macrophages (TAMs), all of which attenuate effector T-cell responses and limit durable tumor control[12,13]. Thus, to improve primary tumor control and elicit abscopal effects of SBRT, there is a need to develop strategies that incorporate agents capable of modulating the radiation-induced immune response.

In this study, we aimed to investigate whether PLAG enhances the antitumor efficacy of radiotherapy in murine tumor models. We systemically evaluated (i) tumor growth inhibition, (ii) $CD8^+$ T-cell infiltration and functional activity, (iii) tumor antigen-specific immune responses, (iv) systemic abscopal effects, and (v) the impact of PLAG on immunosuppressive immune cell populations within the tumor microenvironment. By exploring this novel combination approach, our study provides preclinical evidence supporting PLAG as a potential immunomodulatory adjuvant to radiotherapy.

Materials and methods

Cell cultures

CT-26 murine colorectal carcinoma cells were purchased from American Type Culture Collection (ATCC; VA, USA), and FSaII murine fibrosarcoma were obtained from Dr. Chang W. Song's laboratory (University of Minnesota-Twin Cities, MN, USA). CT-26 cells were maintained in Dulbecco's Modified Eagle's Medium (DMEM, #LM001-05; Welgene Biotech, Korea) supplemented with same 10% fetal bovine serum (FBS, #S001-01; Welgene Biotech) and 1% penicillin-streptomycin (P/S, #15140122; Gibco, USA). FSaII cells were cultured and maintained in RPMI 1640 medium (#LM011-01; Welgene Biotech) supplemented with same ratio of FBS and P/S. 0.5% Trypsin-EDTA (1X) (#15400054; Gibco, Thermo Fisher Scientific Inc.) solution was used for cell detachment. All cells were incubated in a humidified 5% CO_2 incubator at 37℃.

Animal study

All animal experiments were conducted in accordance with institutional animal care guidelines and received ethical approval from the Institutional Animal Care and Use Committee of the Korea Institute of Radiological and Medical Sciences (IACUC-KIRAMS, Seoul, Korea) under the following approval number: Kirams 2022-0085, Kirams2023-0079, Kirams2023-0130, Kirams2023-0132, and Kirams2023-0137. This study conducted in compliance with the ARRIVE guidelines for animal experiments (http://arriveguidelines.org). Male C3H mice and female BALB/c mice (5–6 weeks old) were purchased from the Orient Bio Company. The mice underwent at least one week of acclimatized period before use followed by set of guidelines of the institution. Mice were housed in the animal room with suitable temperature (22 ± 3℃) and humidity (50 ± 20%) and food (Purina) and purified water were provided every 2–3 days.

To establish the mouse syngeneic model, 2×10^5 cells of CT-26 and FSaII were counted and subcutaneously injected into the right hind legs of immunocompetent BALB/c or C3H mice, respectively. Tumor-bearing mice were irradiated when tumors reached a volume between 70 and 100 mm^3, which is approximately 7–10 days after injecting cancer cells. The tumor size was evaluated twice a week using caliper, and the tumor volumes were calculated using the following formula: length (longest diameter) × width (shortest diameter) × height X 0.523 The body weight of the mice was measured once or twice a week using a digital balance.

For irradiating tumors located in hind leg, the mice were anesthetized with an intraperitoneal injection of a 60–80 µl of mixed solution of Alfaxan and Rompun (10:1). The tumor-bearing legs were firmly fixed on the customized board and locally irradiation using a ^{60}Co irradiation unit (Thermatron 780, Atomic Energy of Canada) at a dose rate of 1.0 Gy/minute. Both FSaII and CT-26 tumors were irradiated 7 Gy in two consecutive days, with the total dose of 14 Gy.

PLAG (EC-18; Enzychem life sciences, Korea) was administered orally at a dose of 250 mg/kg, a concentration selected based on previous preclinical studies demonstrating efficacy and safety[19]. Treatment was initiated on the same day as the first irradiation and continued once daily until sacrifice.

Euthanasia was carried out by CO_2 asphyxiation when tumor burden and the general condition of the mice met the predefined humane endpoints. The CO_2 flow rate was maintained at 30–70% of the chamber volume per minute to minimize distress. Death was verified by the absence of respiration and heartbeat. All procedures were performed in accordance with institutional ethical guidelines to ensure the welfare and humane treatment of the experimental animals.

IFN-γ elispot assay

When CT-26-bearing mice were sacrificed 10 and 15 days after the first irradiation, spleens were excised and obtained splenocytes. To obtain the splenocytes of the mice, spleens were cut into small pieces and smashed on the 100-μm filtered strainers (Corning, USA). The red blood cells were lysed using 1X RBC buffer (#R7757; Sigma-Aldrich). The splenocytes (1×10^5 cells/well) and 30 Gy irradiated CT-26 cells (1×10^5 cells/well) were co-cultured on anti-IFN-γ mAb-coated plates (#3321-4 AST-2; Mab tech) and incubated for 72 h at 37℃. Next part of the procedures was performed according to the manufacturer's protocols. The cytokine spots of IFN-γ were detected and counted using an ELISpot Reader System (AID iSPOT ELR07IFL).

Flow cytometry

Subcutaneous FSaII and CT-26 tumors were harvested from mice on day 10 after the first irradiation treatment. Tumors were processed using a tumor dissociation enzyme kit (Miltenyi Biotec, Germany) for 1 h at 37℃ according to the provided manufacturer's protocol, and homogenized using a Gentle MACS dissociator (Miltenyi Biotec, Germany). The dissociated tumor cells were passed through a 100-μm filtered strainer (Corning) to achieve a single-cell suspension suitable for flow cytometry analysis. To block non-specific binding, the single-cell suspensions were incubated with anti-mouse CD16/32 antibodies and stained with each fluorescence labeled antibodies. To assess T-cell function, cells were stimulated with Cell Stimulation Cocktail plus protein transport inhibitors (#00–4975-93; Invitrogen) at 37℃ 2 h. Following stimulation, cells were stained with IFN-γ (#505808; BioLegend) according to the previously described surface staining protocol. Flow Cytometry data acquisition was performed using a LSRFortessa™ (BD Bioscience) and analyzed using FlowJo software (BD). Absolute cell counts were determined using precision counting beads (#424902; BioLegend).

Quantitative real-time PCR (qRT-PCR)

Total RNA was extracted from tumor tissues using Tri-RNA reagent (FATRR001; FAVORGEN, Taiwan), following the manufacturer's protocol. 1 μg of RNA was reverse transcribed into cDNA using the SensiFAST cDNA synthesis Kit (#BIO-65054; Meridian Bioscience, Newtown, OH, USA). The resulting cDNA was diluted 1:10, and 2 μl of the diluted cDNA was used in a 20 μl quantitative PCR reaction. qRT-PCR was conducted using the KAPA SYBR FAST (#KK4602; Roche, Basel, Switzerland) on a Roche LightCycler® 96 system. The thermal cycling conditions included an initial activation step at 95˚C for 10 min, followed by 45 amplification cycles consisting of denaturation at 95˚C for 15 s and annealing/extension at 60˚C for 1 min. Gene expression levels were normalized at Gapdh as the internal control, and relative expression was quantified using the 2-ΔΔCt method[20]. The primers used in the qRT-PCR targeted mouse genes and are listed as follows:

Gapdh Forward 5'-CGACTTCAACAGCAACTCCCACTCTTCC-3'.
Reverse 5'-TGGGTGGTCCAGGGTTTCTTACTCCTT-3'.
Il-6 Forward 5'-AACAAGAAAGACAAAGCCAG-3'.
Reverse 5'-GGAGAGCATTGGAAATTGG-3'.
Tgfβ1 Forward 5'-CAAGGGCTACCATGCCAACT-3'.
Reverse 5'-GTACTGTGTGTCCAGGCTCCAA-3'.
Arg1 Forward 5'-CAGAAGAATGGAAGAGTCAG-3'.
Reverse 5'-CAGATATGCAGGGAGTCACC-3'.
Cd274 (PD-L1) Forward 5'-GGCATTTGCTGAACGCAT-3'.
Reverse 5'-CAATTAGTGCAGCCAGGT-3'.

Statistical analysis

Statistical analyses were performed using GraphPad Prism software (version 9) unless otherwise stated. Tumor growth delay graphs were obtained using 2-way ANOVA analysis of variance, wile one-way ANOVA was used when comparing multiple groups. And 2-tailed Student's t-test was used to analyze the statistical differences between two groups. Statistical significance was defined as a p−value less than 0.05. All data are presented as the mean ± standard error of the mean (SEM).

Results

PLAG augments the antitumor efficacy of radiotherapy in an immune-dependent manner

To test our hypothesis that PLAG enhances radiotherapy-induced antitumor immunity without body weight loss, tumor growth and body weight were evaluated in immunocompetent murine models. In both CT-26-bearing BALB/c mice and FSaII-bearing C3H mice, combination treatment with radiotherapy (7 Gy × 2) and PLAG (250 mg/kg/day) resulted in a significant delay of tumor progression compared with radiotherapy or PLAG alone (Fig. 1A and B left). Importantly, no significant body weight loss was observed across all treatment groups (Fig. 1A and B right).

In contrast, in immunodeficient BALB/c-nude mice, radiotherapy alone and radiotherapy combined with PLAG showed no significant differences in tumor growth or body weight changes (Fig. 1C). The absence of therapeutic benefit from PLAG in immune cell deficient hosts indicates that the antitumor efficacy observed in immunocompetent mice is critically dependent on adaptive immune responses rather than direct cytotoxic effects.

PLAG combined with radiotherapy induces functional and systemic antitumor immunity

Given the immune-dependent nature of the observed therapeutic benefit, we next investigated whether radiotherapy combined with PLAG induces a functional and systemic tumor-antigen-specific immune response. IFN-γ ELISpot assay were performed using splenocytes harvested at defined post-treatment time points. In this assay, CT-26 cells irradiated with 30 Gy were used solely as a source of tumor antigen, enabling assessment of

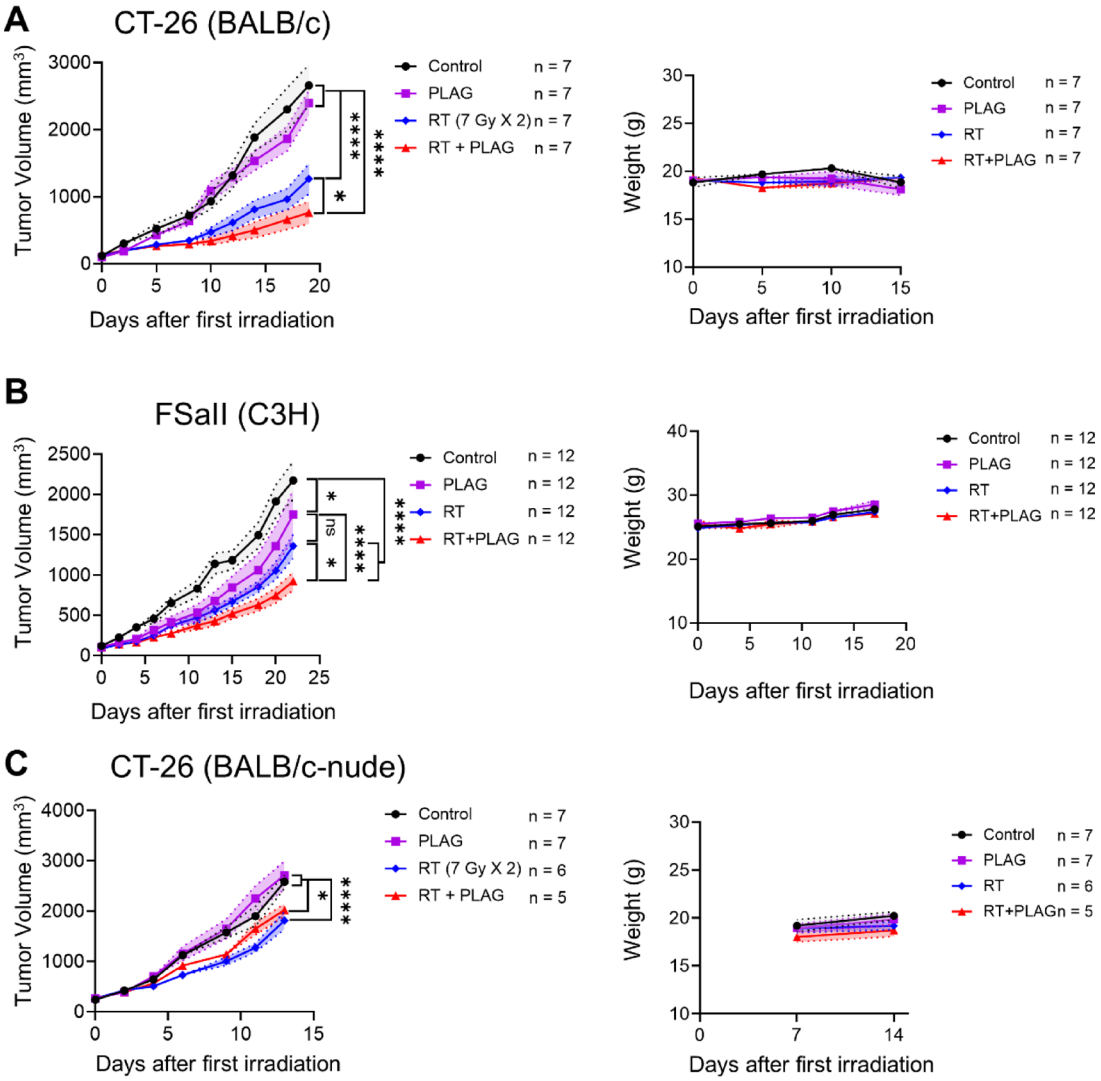

Fig. 1. PLAG improves the antitumor efficacy of radiotherapy without inducing systemic toxicity in CT-26 and FSaII tumor models. All tumor-bearing mice were treated with saline, PLAG (250 mg/kg/day, daily, oral injection), radiotherapy (RT, 7 Gy × 2), or the combination of PLAG and RT. Tumor volumes were measured over time (left). Body weights were monitored during treatment to evaluate systemic toxicity (right). **(A)** CT-26 tumor-bearing BALB/c mice ($n = 7$ per group), **(B)** FSaII tumor-bearing C3H mice ($n = 12$ per group), and **(C)** CT-26 tumor-bearing BALB/c-nude immunodeficient mice (control $n = 7$, PLAG $n = 7$, RT $n = 6$, RT + PLAG $n = 5$). Growth curve data are presented as mean ± standard error of the mean with a two-way ANOVA analysis of variance with Sidak's multiple comparison at the endpoint, respectively. *$P < .05$, **** $P < .0001$.

antigen-specific IFN-γ secretion by splenic T-cells rather than direct cytotoxic effects. Splenocytes isolated from CT-26-bearing mice on days 10 and 15 after first radiotherapy (7 Gy × 2) showed no significant IFN-γ secretion in the absence of antigen stimulation. However, upon exposure to irradiated tumor cell-derived antigens, splenocytes from the radiotherapy plus PLAG group exhibited a robust increase in tumor antigen-specific IFN-γ-secreting cells compared with all other groups (Fig. 2A). These findings indicate that PLAG, when combined with radiotherapy, promotes a functional and systemic antitumor immune response.

PLAG enhances functional activation of tumor-infiltrating CD8⁺ T-cells

Because the therapeutic benefit of the combination treatment was associated with systemic tumor antigen-specific immune activation (Fig. 2A), we next investigated whether PLAG modulates tumor-infiltrating immune populations in immunocompetent hosts. Flow cytometric analysis of CT-26 tumors harvested on day 10 after irradiation revealed that the total number of intratumoral $CD8^+$ T-cells was comparable among all treatment groups (Fig. 3A), indicating that PLAG did not primarily affect $CD8^+$ T-cell recruitment into tumors. Functional profiling demonstrated a marked increase in IFN-γ^+ and Granzyme B (GzmB)$^+$ $CD8^+$ T-cells in the radiotherapy plus PLAG group compared with radiotherapy alone, whereas TNF-α^+ $CD8^+$ T-cells remained unchanged (Fig. 3A). Furthermore, the combination treatment significantly increased the number of effector memory $CD8^+$ T-cells ($IL7R\alpha^+CD44^+CD62L^-$), without affecting naïve ($IL7R\alpha^+CD44^-CD62L^+$) and central memory

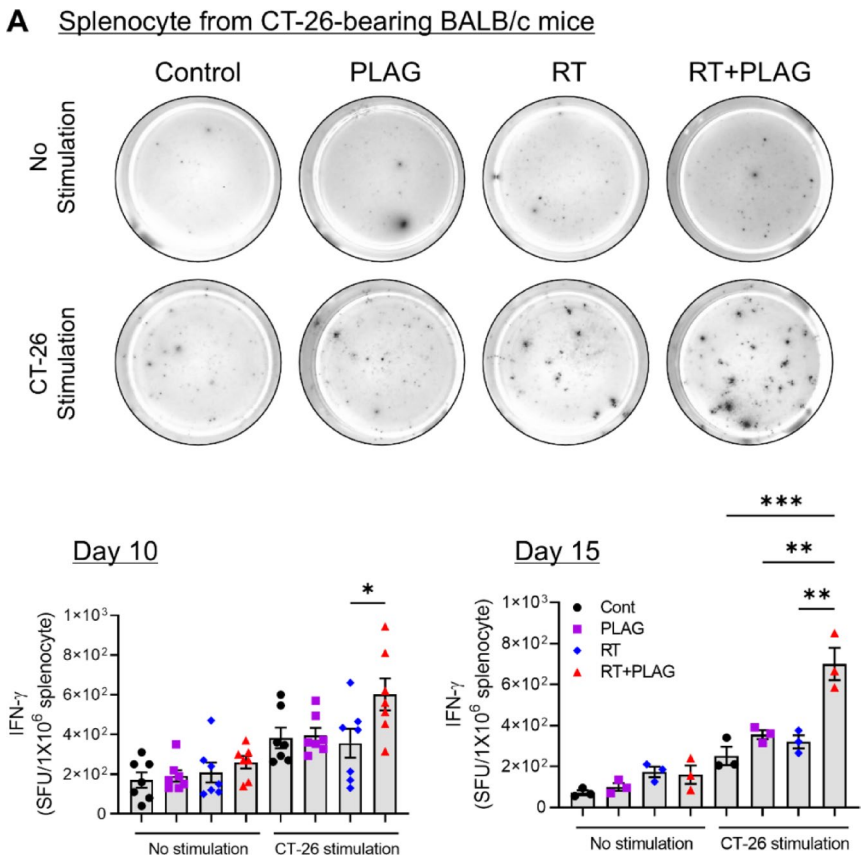

Fig. 2. PLAG in combination with radiotherapy augments tumor antigen-specific IFN-γ production in splenocytes of tumor-bearing mice. (A) Splenocytes from CT-26-bearing mice were isolated on day 10 ($n = 7$ per group) and day 15 ($n = 3$ per group) post-irradiation and co-cultured with irradiated tumor cell lysates (30 Gy) for 72 h. ELISpot assay was performed to quantify tumor antigen-specific IFN-γ-secreting cells. Representative images and quantification of IFN-γ spots are shown. Data represent mean ± SEM of spot-forming units per 1×10^5 cells. Data are shown as mean ± standard error of the mean with a one-way ANOVA. $^*P < .05$.

(IL7Rα$^+$CD44$^+$CD62L$^+$) subsets (Fig. 3B). The gating strategies used for these analyses are shown in Fig. 3C. By contrast, neither the total number of CD4$^+$ T-cells nor the number of IFN-γ-producing CD4$^+$ T-cells was significantly increased by the addition of PLAG to radiotherapy (Fig. 3D). Together, these findings suggest that the enhanced tumor antigen-specific IFN-γ responses observed at the systemic level (Fig. 2A) are predominantly attributable to functional activation of CD8$^+$ T-cells rather than CD4$^+$ T-cells.

Collectively, these results indicate that PLAG preferentially promotes functional differentiation and cytotoxic capacity of tumor-infiltrating CD8$^+$ T-cells rather than increasing their absolute numbers, suggesting a qualitative shift toward an effector-dominant immune response within irradiated tumors.

PLAG could not reduce the immunosuppressive cell populations within tumors under these experimental conditions evaluated

To determine whether the antitumor immune responses induced by the combination of radiotherapy and PLAG were associated with modulation of immunosuppressive myeloid populations, we focused our analysis on myeloid-derived suppressor cells (MDSCs), which have been reported to impair CD8$^+$ T-cell function on day 10 after 1-day interval radiotherapy[21]. Flow cytometric analysis performed on day 10 after irradiation revealed no significant differences in the numbers of M-MDSCs or PMN-MDSCs between the radiotherapy-alone and the combined with radiotherapy and PLAG groups (Fig. 4A). The number of iNOS-expressing MDSCs, a key functional suppressive subset, was not increased following combination treatment (Fig. 4B). Unexpectedly, PD-L1 expression on MDSCs showed an increasing trend in the combination treatment group compared with radiotherapy alone (Fig. 4C). These data suggest that PD-L1 upregulation on MDSCs in tumors treated with radiotherapy plus PLAG does not translate into dominant immunosuppressive activity sufficient to counteract CD8$^+$ T-cell-mediated antitumor responses (Fig. 2A).

Analysis of immunosuppressive gene expression within the tumor microenvironment demonstrated that although IL-6 expression was significantly increased in the radiotherapy-alone group compared with the PLAG-alone group, no significant differences were observed between the radiotherapy-alone and combination groups for IL-6, TGF-β, ARG1, and PD-L1 (Fig. 4D). Furthermore, no significant quantitative changes were observed

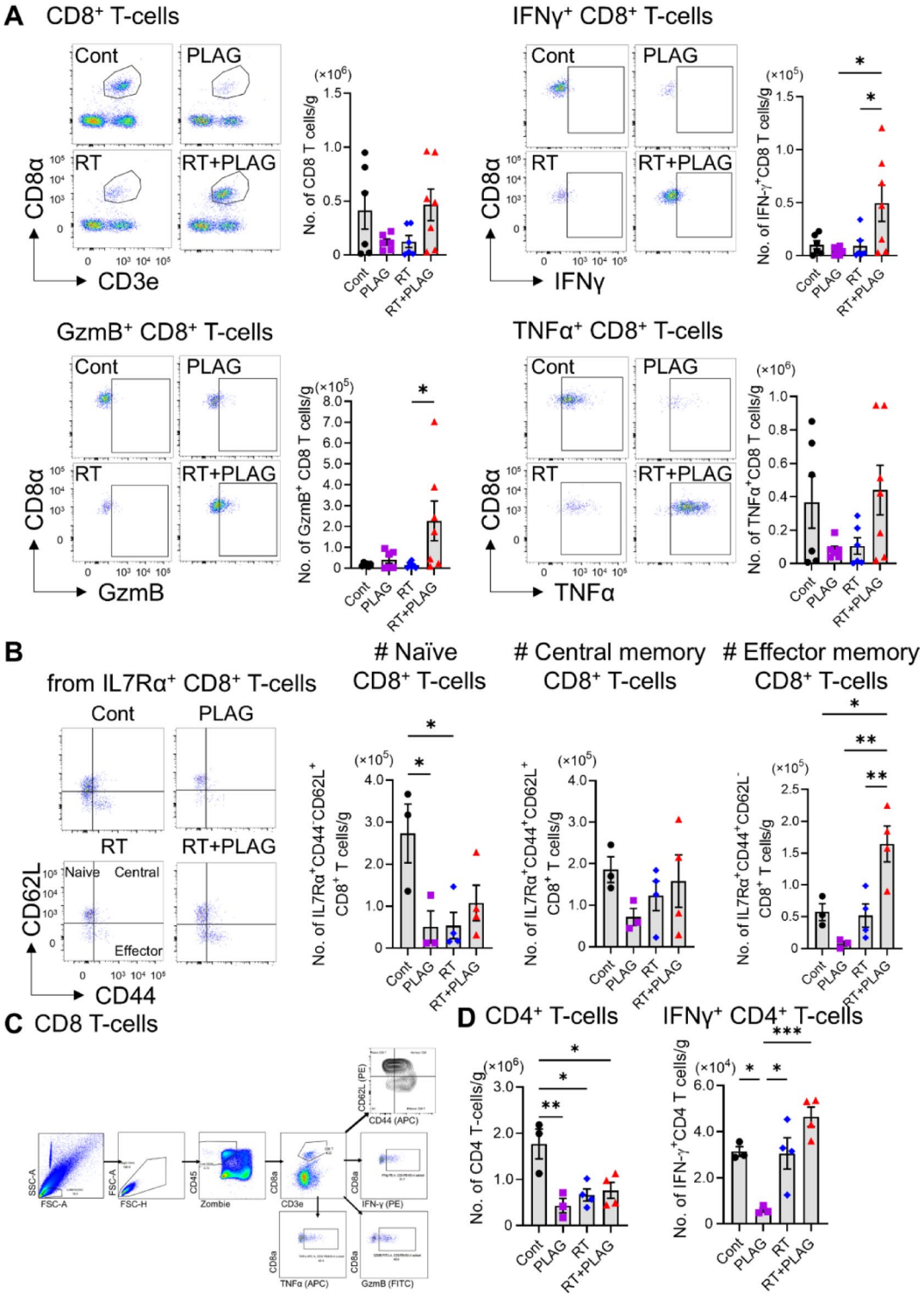

Fig. 3. PLAG promotes infiltration and activation of CD8⁺ T cells in irradiated CT-26 tumors. **(A)** Tumors were harvested from CT-26-bearing BALB/c mice on day 10 post-irradiation and analyzed by flow cytometry. Total CD8⁺ T-cell counts and the number of IFN-γ⁺, Granzyme B⁺, and TNF-α⁺ CD8⁺ T-cells were evaluated. $n = 6–7$ mice per group. **(B)** Memory phenotypes of CD8⁺ T-cells were assessed based on IL-7Rα, CD44, and CD62L expression. Effector memory (IL-7Rα⁺CD44⁺CD62L⁻), central memory (IL-7Rα⁺CD44⁺CD62L⁺), and naïve (IL-7Rα⁺CD44⁻CD62L⁺) subsets were quantified. ($n = 3–4$ mice per group). **(C)** Flow cytometry gating strategy for CD8⁺ T-cells and effector CD8⁺ T-cells **(D)** Total CD4⁺ T-cell counts and the number of IFN-γ⁺ CD4⁺ T-cells were evaluated. ($n = 3–4$ mice per group). Data are shown as mean ± standard error of the mean with a one-way ANOVA. $^{*}P < .05$, $^{**}P < .01$.

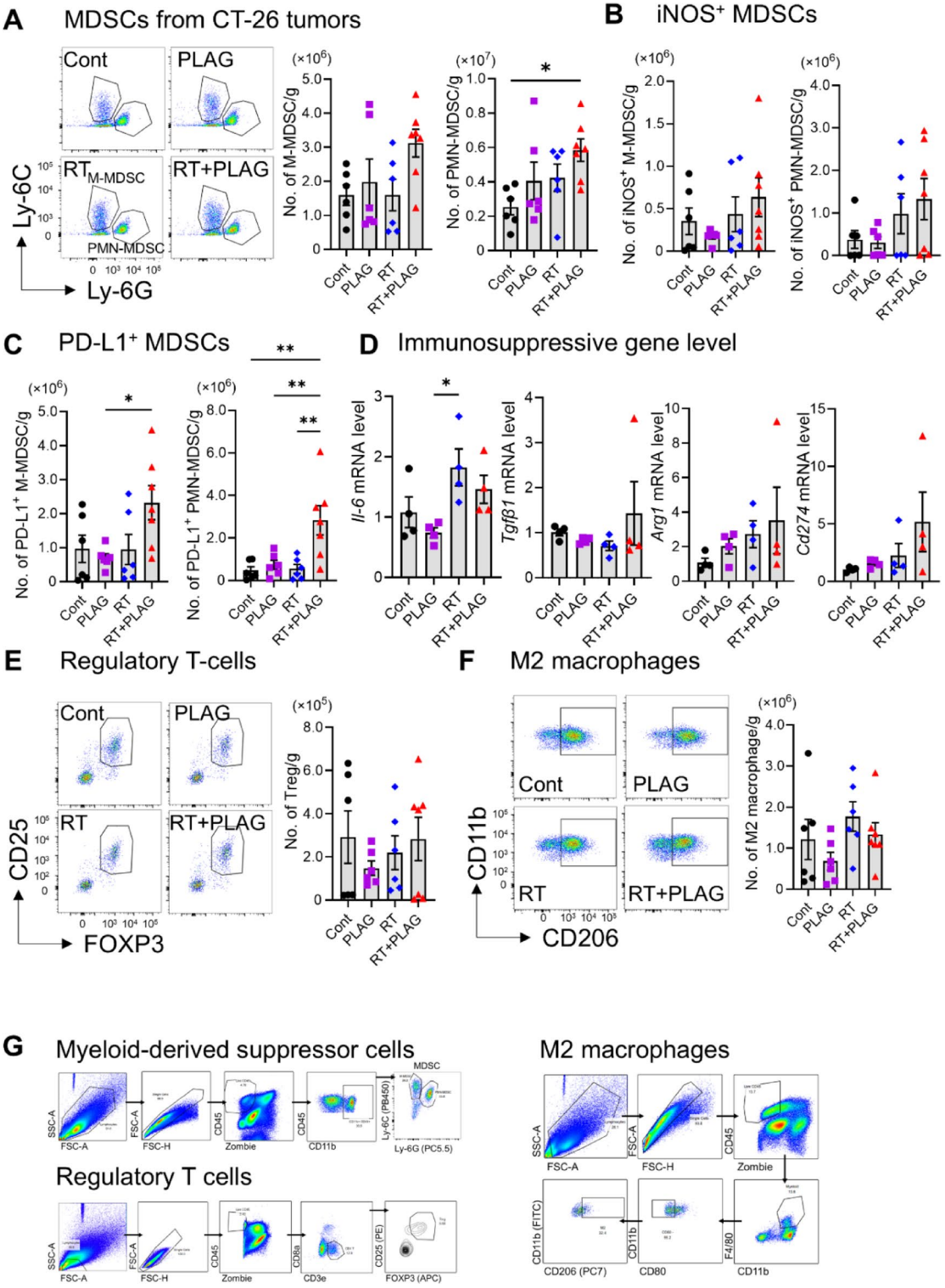

Fig. 4. Flow cytometric analysis of tumor-infiltrating MDSC subsets and functional markers. Tumors were collected from CT-26 tumors on day 10 post-irradiation. Flow cytometry was performed to assess the number of tumor-infiltrating **(A)** M-MDSCs ($CD11b^{+}Ly\text{-}6C^{high}Ly\text{-}6G^{low}$), and PMN-MDSCs ($CD11b^{+}Ly\text{-}6C^{low}Ly\text{-}6G^{high}$), **(B)** $iNOS^{+}$ MDSCs, and **(C)** PD-$L1^{+}$ MDSCs. ($n = 6$–7 mice per group) **(D)** Bar graphs showed the qRT-PCR results. CT-26 tumors were extracted 15 days after radiotherapy for qRT-PCR experiments. mRNA expression of Il-6, Tgfβ1, Arg1, and Cd274 (PD-L1) in tumor mass. ($n = 4$ mice per group). **(E)** Tregs ($CD3^{+}CD4^{+}FOXP3^{+}CD25^{+}$) and **(F)** M2 macrophages ($CD11b^{+}CD80^{-}CD206^{+}$). ($n = 6$–7 mice per group). **(G)** Flow cytometry gating strategy for MDSCs, Tregs, and M2 macrophages. Data are shown as mean ± standard error of the mean with a one-way ANOVA. $^{*}P < .05$, $^{**}P < .01$.

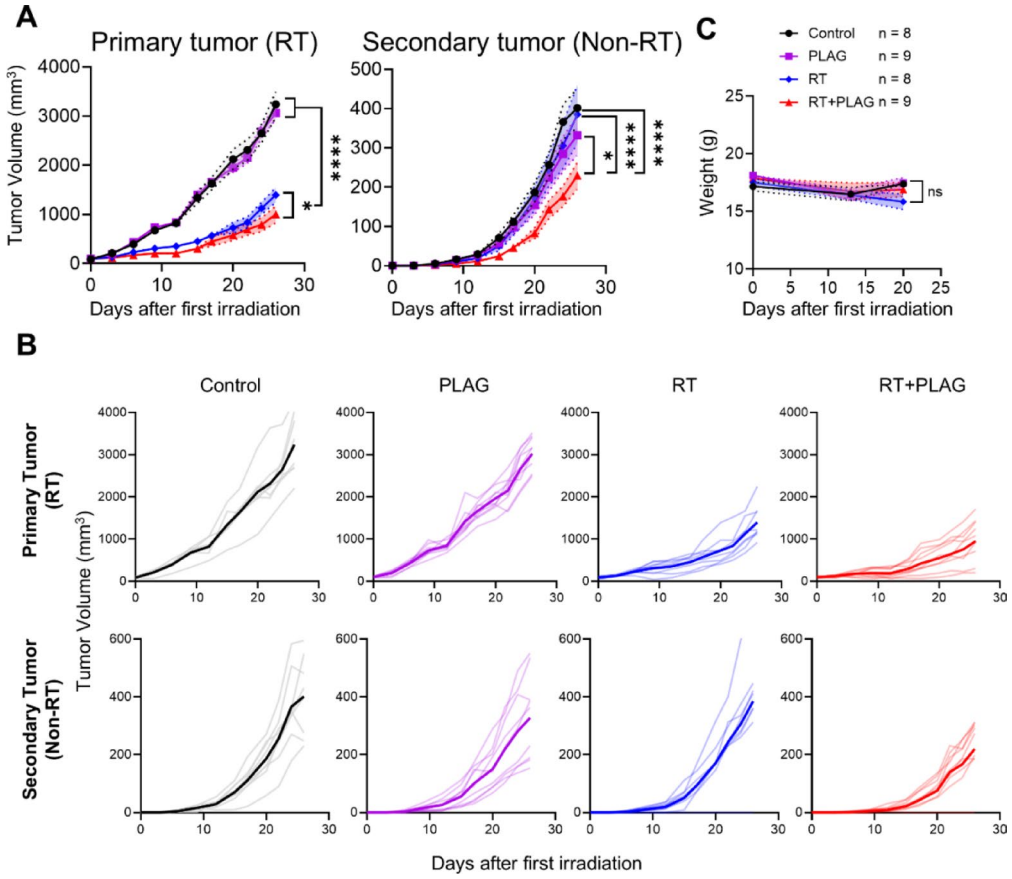

Fig. 5. PLAG enhances the abscopal effect of radiotherapy, leading to suppression of both irradiated primary and distant non-irradiated tumors. A bilateral CT-26 tumor model was established, and only the primary tumor was irradiated (7 Gy × 2). Mice were treated with saline, PLAG, RT, or a combination of RT and PLAG (control $n = 8$, PLAG $n = 9$, RT $n = 8$, RT + PLAG $n = 9$). **(A)** Growth curves of primary tumors (irradiated) and secondary tumors (non-irradiated) are shown. Combination treatment significantly delayed growth in both sites. **(B)** Individual tumor growth curve of secondary tumors. The bold line indicates the mean tumor volume of each group, and the faint lines represent individual tumor growth. **(C)** Body weights were monitored during treatment to evaluate systemic toxicity. All data are presented as mean ± standard error of the mean with a two-way ANOVA analysis of variance with Sidak's multiple comparison at the endpoint, respectively. *$P < .05$, ** $P < .01$, ****$P < .0001$.

in other immunosuppressive populations, including regulatory T cells (Tregs) and M2 macrophages, across treatment groups (Fig. 4E and F). The gating strategies used to identify MDSCs, Tregs, and M2 macrophages are shown in Fig. 4G. These findings could not show the proof that PLAG would enhance radiotherapy efficacy by reducing immunosuppressive cell populations within tumors, further study is necessary.

PLAG combined with radiotherapy promotes effective abscopal tumor control

Given that PLAG augmented radiotherapy-induced systemic and functional antitumor immune responses without altering immunosuppressive cell populations, we next investigated whether this immune activation translated into functional control of distant, non-irradiated tumors. To address this, a two-site CT-26 tumor model was established, in which the primary tumor implanted in the right hind thigh was selectively irradiated, while a secondary tumor implanted at a distant anatomical site (dorsal region) was left unirradiated. In this model, combination treatment with radiotherapy and PLAG resulted in sustained suppression of irradiated primary tumors (Fig. 5A left and 5B upper). Notably, growth of secondary non-irradiated tumors was also significantly inhibited in the radiotherapy plus PLAG group compared with all other treatment groups ($P < .0001$), whereas radiotherapy alone failed to exert a comparable effect (Fig. 5A right and 5B below). No significant change in body weight was observed (Fig. 5C). These findings indicate that PLAG enhances radiotherapy-induced systemic antitumor immunity sufficient to mediate effective abscopal tumor control.

Taken together, these results demonstrate that PLAG amplifies radiotherapy-induced tumor antigen-specific systemic antitumor immune responses, translating into robust abscopal control of distant, non-irradiated tumors. These findings support the potential clinical applicability of PLAG as an immune-modulating adjuvant to radiotherapy that improves antitumor efficacy.

Discussion

In this study, we demonstrated that PLAG significantly enhances the therapeutic efficacy of radiotherapy in murine tumors without treatment associated body weight loss. And the observed antitumor effects are not attributable to direct cytotoxicity of PLAG, but rather to the amplification of radiotherapy-induced antitumor immune responses. This is supported by the complete loss of therapeutic benefit in immunodeficient BALB/c-nude mice, indicating that an intact adaptive immune system is essential for the efficacy of PLAG combined with RT. To our knowledge, this study provides the first evidence that PLAG modulates immune responses induced by high dose radiotherapy and enhances antitumor efficacy not only at the primary tumor but also at distant not-irradiated sites, consistent with the induction of an abscopal effect.

Radiotherapy has been reported to enhance $CD8^+$ T-cell infiltration, which effect is highly dependent on radiation dose, fractionation schedule, tumor type, and timing of immune analysis[22–24]. Especially, in our previous work, optimization of the fractionation schedule enhances the efficacy of radiotherapy by increasing $CD8^+$ T-cell infiltration, a phenomenon closely associated with immunosuppressive cell populations, particularly myeloid-derived suppressor cells (MDSCs)[21]. Importantly, our findings emphasized that the functional quality of $CD8^+$ T-cells, rather than their absolute numbers, plays a critical role in mediating antitumor immunity. In addition, we repositioned low-dose cyclophosphamide (Cy) as a radioimmunomodulatory agent and demonstrated that its immunostimulatory effects are mediated through dendritic cell stimulation. Given these prior observations, which showed that modulation of fractionation schedules or immune regulation can enhance radiotherapy efficacy, we investigated the immunomodulatory effects of PLAG in combination with radiotherapy. While, in the present study, PLAG plus radiotherapy selectively enhanced the functional quality of $CD8^+$ T-cells, as evidenced by increased numbers of INF-γ^+, Granzyme B^+, and effector memory $CD8^+$ T-cell subsets, without significantly altering the total number of $CD8^+$ T-cell infiltration in tumors. These findings indicate that PLAG induced functional reprogramming and differentiation of tumor-infiltrating $CD8^+$ T-cells rather than their numerical expansion. This qualitative enhancement of $CD8^+$ T-cell function was further supported by ELISpot assays (Fig. 2A), which demonstrated a marked increase in tumor antigen-specific IFN-γ-secreting splenocytes in the radiotherapy plus PLAG group. Importantly, tumor antigen-specific IFN-γ responses were elevated at day 10 and further increased by day 15, suggesting that continued administration of PLAG sustains and amplifies systemic antitumor immune activation following radiotherapy. This temporal pattern closely coincided with the emergence of a robust abscopal effect, highlighting that the combination therapy effectively suppressed not only irradiated primary tumors but also distant, non-irradiated secondary tumors. While, PLAG alone failed to exert comparable control over secondary tumor growth, suggesting that PLAG requires radiotherapy-induced immune priming to achieve systemic antitumor effects. Therefore, the present study demonstrates that PLAG appears to enhance high dose radiotherapy-induced antitumor immunity.

Regarding to PLAG, previous studies have established the immunomodulatory effects of PLAG across multiple disease models. In radiation injury models, a 250 mg/kg dose of PLAG promoted epithelial regeneration and preserved mucosal integrity by modulating necroptosis and regulating pathological neutrophil trafficking, including excessive recruitment and prolonged tissue accumulation, resulting in improved survival in gastrointestinal ARS models[3]. In tumor settings combined with immune checkpoint blockade such as anti-PD-1 or anti-PD-L1, lower-dose PLAG (100 mg/kg) has been reported to suppress excessive infiltration of Ly-$6G^+$ neutrophil—cells phenotypically similar to PMN-MDSCs—into the tumor microenvironment, alleviating immune suppression and enhancing antitumor effects by promoting $CD8^+$ T-cell tumor-infiltrating[4–6]. Based on these reporting that PLAG immune modulating effect would be neutrophil or PMN-MDSC, we carefully examined whether the enhanced antitumor immunity observed with radiotherapy plus PLAG was associated with modulation of immunosuppressive cell compartments. Contrary to our expectations that PLAG would reduce neither of M-MDSCs, PMN-MDSCs, regulatory T cells, or M2 macrophages, PLAG did not exhibit a significant effect on these cells. And the frequency of iNOS-expressing MDSCs, a key functional suppressive subset, was not decreased following combination treatment. Moreover, PD-L1 expression on MDSCs showed an increasing trend in the radiotherapy plus PLAG group. These findings suggest two possible explanations. The one is that the immunological impact of high-dose PLAG on the temporal immune changes of tumor induced by high dose radiotherapy differs from the PLAG–driven immune modulation reported in ARS. That is a primary driver of PLAG-mediated therapeutic synergy with high-dose radiotherapy would not be associated with immunosuppressive cell. The other is that PLAG-mediated immune suppression after radiotherapy may be temporally dissociated from the time points assessed in the present study. These observations were derived from immune analyses performed at defined post-treatment time points (days 10 and 15), and it is plausible that immune dynamics may differ at earlier or later phases following radiotherapy.

This study provides the first evidence that PLAG synergistically enhances the antitumor efficacy of radiotherapy by promoting functional activation of $CD8^+$ T-cells, augmenting tumor antigen-specific systemic immune responses, and enabling robust abscopal tumor control. In addition, while no treatment-associated body weight loss was observed during the experimental period, long-term and off-target toxicities of PLAG were not evaluated in the present study. Accordingly, future studies incorporating longitudinal temporal profiling, in vitro functional assays of immunosuppressive cells, and transcriptional analyses as well as comprehensive long-term safety assessments will be essential. These findings position PLAG as a promising immunomodulatory adjuvant for high dose radiotherapy-based strategies, such as stereotactic ablative radiotherapy.

Data availability

Research data are available from the corresponding author upon reasonable request.

Received: 7 November 2025; Accepted: 13 January 2026

Published online: 24 February 2026

References

1. Hwang, H. J. et al. Effect of 1-palmitoyl-2-linoleoyl-3-acetyl-rac-glycerol on immune functions in healthy adults in a randomized controlled trial. *Immune Netw.* **15**, 150–160. https://doi.org/10.4110/in.2015.15.3.150 (2015).
2. Yang, H. O. et al. Purification and structural determination of hematopoietic stem cell-stimulating monoacetyldiglycerides from cervus Nippon (deer antler). *Chem. Pharm. Bull. (Tokyo).* **52**, 874–878. https://doi.org/10.1248/cpb.52.874 (2004).
3. Jeong, J. et al. Mitigating the effects of 1-Palmitoyl-2-linoleoyl-3-acetyl-rac-glycerol on Gastrointestinal acute radiation syndrome after Total-Body irradiation in mice. *Radiat. Res.* **202**, 706–718. https://doi.org/10.1667/RADE-24-00126.1 (2024).
4. Kim, G. et al. 1-palmitoyl-2-linoleoyl-3-acetyl-rac-glycerol treatment inhibits abnormal tumor growth by regulating neutrophil infiltration in a non-small cell lung carcinoma mouse model. *Biomed. Pharmacother.* **178**, 117269. https://doi.org/10.1016/j.biopha.2024.117269 (2024).
5. Kim, G. T. et al. Improving anticancer effect of aPD-L1 through Lowering neutrophil infiltration by PLAG in tumor implanted with MB49 mouse urothelial carcinoma. *BMC Cancer.* **22**, 727. https://doi.org/10.1186/s12885-022-09815-7 (2022).
6. Lee, H. R. et al. 1-Palmitoyl-2-Linoleoyl-3-Acetyl-rac-Glycerol (PLAG) rapidly resolves LPS-Induced acute lung injury through the effective control of neutrophil recruitment. *Front. Immunol.* **10**, 2177. https://doi.org/10.3389/fimmu.2019.02177 (2019).
7. Henson, C. et al. A Two-Stage phase 2, Multicenter, Randomized, Double-Blind, Placebo-Controlled study to evaluate the safety and efficacy of Ec-18 in altering the severity and course of oral mucositis secondary to chemoradiation therapy for squamous cell cancers of the head and neck. *Cancers (Basel).* 17. https://doi.org/10.3390/cancers17101663 (2025).
8. Kim, Y. J. et al. Mitigation of hematopoietic syndrome of acute radiation syndrome by 1-Palmitoyl-2-linoleoyl-3-acetyl-rac-glycerol (PLAG) is associated with regulation of systemic inflammation in a murine model of Total-Body irradiation. *Radiat. Res.* **196**, 55–65. https://doi.org/10.1667/RADE-20-00288.1 (2021).
9. Song, C. W. et al. Reoxygenation and repopulation of tumor cells after ablative hypofractionated radiotherapy (SBRT and SRS) in murine tumors. *Radiat. Res.* **192**, 159–168 (2019).
10. Timmerman, R. et al. Stereotactic body radiation therapy for inoperable early stage lung cancer. *JAMA* **303**, 1070–1076. https://doi.org/10.1001/jama.2010.261 (2010).
11. Reynders, K., Illidge, T., Siva, S., Chang, J. Y. & De Ruysscher, D. The abscopal effect of local radiotherapy: using immunotherapy to make a rare event clinically relevant. *Cancer Treat. Rev.* **41**, 503–510. https://doi.org/10.1016/j.ctrv.2015.03.011 (2015).
12. Bernstein, M. B., Krishnan, S., Hodge, J. W. & Chang, J. Y. Immunotherapy and stereotactic ablative radiotherapy (ISABR): a curative approach? *Nat. Rev. Clin. Oncol.* **13**, 516–524. https://doi.org/10.1038/nrclinonc.2016.30 (2016).
13. Akanda, Z. Z. et al. A narrative review of combined stereotactic ablative radiotherapy and immunotherapy in metastatic non-small cell lung cancer. *Transl Lung Cancer Res.* **10**, 2766–2778. https://doi.org/10.21037/tlcr-20-1117 (2021).
14. Masucci, G. V., Wersall, P., Kiessling, R., Lundqvist, A. & Lewensohn, R. Stereotactic ablative radio therapy (SABR) followed by immunotherapy a challenge for individualized treatment of metastatic solid tumours. *J. Transl Med.* **10**, 104. https://doi.org/10.1186/1479-5876-10-104 (2012).
15. Moreno-Olmedo, E. et al. The Landscape of Stereotactic Ablative Radiotherapy (SABR) for Renal Cell Cancer (RCC). *Cancers (Basel).* **16** (2024). https://doi.org/10.3390/cancers16152678
16. Song, C. W. et al. Biological principles of stereotactic body radiation therapy (SBRT) and stereotactic radiation surgery (SRS): indirect cell death. *Int. J. Radiat. Oncol. Biol. Phys.* **110**, 21–34. https://doi.org/10.1016/j.ijrobp.2019.02.047 (2021).
17. Rodriguez-Ruiz, M. E., Vitale, I., Harrington, K. J., Melero, I. & Galluzzi, L. Immunological impact of cell death signaling driven by radiation on the tumor microenvironment. *Nat. Immunol.* **21**, 120–134. https://doi.org/10.1038/s41590-019-0561-4 (2020).
18. McLaughlin, M. et al. Inflammatory microenvironment remodelling by tumour cells after radiotherapy. *Nat. Rev. Cancer.* **20**, 203–217. https://doi.org/10.1038/s41568-020-0246-1 (2020).
19. Lee, H. R. et al. The therapeutic effect of PLAG against oral mucositis in hamster and mouse model. *Front. Oncol.* **6**, 209. https://doi.org/10.3389/fonc.2016.00209 (2016).
20. Livak, K. J. & Schmittgen, T. D. Analysis of relative gene expression data using real-time quantitative PCR and the 2(-Delta delta C(T)) method. *Methods* **25**, 402–408. https://doi.org/10.1006/meth.2001.1262 (2001).
21. Kim, H. et al. Five-Day spacing of two fractionated ablative radiotherapies enhances antitumor immunity. *Int. J. Radiat. Oncol. Biol. Phys.* **118**, 498–511. https://doi.org/10.1016/j.ijrobp.2023.09.014 (2024).
22. Lin, L. et al. High-dose per fraction radiotherapy induces both antitumor immunity and immunosuppressive responses in prostate tumors. *Clin. Cancer Res.* **27**, 1505–1515. https://doi.org/10.1158/1078-0432.CCR-20-2293 (2021).
23. Grapin, M. et al. Optimized fractionated radiotherapy with anti-PD-L1 and anti-TIGIT: a promising new combination. *J. Immunother Cancer.* **7**, 160. https://doi.org/10.1186/s40425-019-0634-9 (2019).
24. Kim, H. et al. Low-Dose cyclophosphamide enhances the tumoricidal effects of 5-Day spacing stereotactic ablative radiotherapy by boosting antitumor immunity. *Cancer Res. Treat.* **57**, 678–692. https://doi.org/10.4143/crt.2024.807 (2025).

Acknowledgements

We acknowledge Enzychem Life Sciences for providing PLAG and funding support for this study.

Author contributions

Conceived and designed the analysis: Hyunkyung Kim, Haeun Cho, Seok-Joo Chun, Mi-Sook KimConducted the experiment: Hyunkyung Kim, Haeun Cho, Sojung Sun, Tae-Jin KimContributed data or analysis tools: Hyunkyung Kim, Haeun Cho, Sojung Sun, Tae-Jin KimPerformed the analysis: Hyunkyung Kim, Haeun Cho, Sojung SunWrote the paper: Hyunkyung Kim, Haeun Cho, Mi-Sook KimRevised the paper: Tae-Jin Kim, Kwangmo Yang, Won Il Jang, Seok-Joo Chun.

Funding

This research was supported by the Korea Institute of Radiological & Medical Sciences (KIRAMS, Seoul, Korea) (No.51299 – 2023, 50552 – 2025).

Declarations

Competing interests

The authors declare no competing interests.

Ethical approval

Mice were housed in particular pathogen-free facilities. All investigations involving mice have been carried out in line with the applicable ethical standards for animal testing and research as well as the Institutional Animal Care and Use Committee of Korea Institute of Radiological and Medical Sciences (IACUC-KIRAMS, Seoul, Korea) -approved protocols (Kirams 2022-0085, Kirams2023-0079, Kirams2023-0130, Kirams2023-0132, and Kirams2023-0137).

Additional information

Correspondence and requests for materials should be addressed to M.-S.K.

Reprints and permissions information is available at www.nature.com/reprints.

Publisher's note Springer Nature remains neutral with regard to jurisdictional claims in published maps and institutional affiliations.